

Comparison of Experimental and Calculated Hyperfine Coupling Constants. Which Radicals Are Formed in Irradiated Guanine?

Stacey D. Wetmore and Russell J. Boyd*

Department of Chemistry, Dalhousie University, Halifax, NS B3H 4J3, Canada

Leif A. Eriksson

Department of Quantum Chemistry, Uppsala University, Box 518, Uppsala, Sweden, 751 20

Received: June 2, 1998; In Final Form: August 24, 1998

The geometries, spin density distributions, and hyperfine coupling constants (HFCC) in possible radiation products of guanine are studied through the use of density functional theory. Numerous hydrogenated, dehydrogenated, and hydroxylated radicals are examined and the coupling constants are compared to those obtained from detailed ESR/ENDOR studies on single crystals of different guanine derivatives. The calculated couplings for the guanine anion deviate from those observed experimentally. The possibility that the radical assigned experimentally to the guanine anion may in fact be guanine hydrogenated at the O6 position is discussed. The anion and its O6 protonated form can be distinguished through the experimental determination of the amino hydrogen couplings. The HFCCs calculated for the guanine cation radical do not match the experimental results. In contrast with the results for the guanine anion and cation, theory and experiment agree well for many of the observed hydrogenated and dehydrogenated radical products. Various N7-protonated guanine radicals are also examined. The extent of disagreement between experiment and high-level theoretical calculations for many of the N7-protonated guanine radicals suggests that further experimental and theoretical investigations of these radiation products are desirable.

Introduction

Early investigations of the effects of radiation on DNA speculated that initially only two main products are formed, namely the thymine anion and the guanine cation.^{1–4} Later studies indicated that the cytosine anion may also play an important role in the capture of an electron in full DNA samples.^{5,6} The various cations and anions, proposed to be initially created upon radiation, are known to undergo deprotonation or protonation, respectively. The end products of radiated DNA exist as DNA–protein cross-links^{7–9} and/or single strand breaks.¹⁰

Many experimental investigations on the products of irradiated DNA have evolved around single-crystal studies performed on the four DNA bases in numerous crystalline environments.¹¹ In addition, some recent work has concentrated on radiation effects on the DNA base pairs.^{12,13} The key experimental techniques implemented are electron spin resonance (ESR) and the more sophisticated electron nuclear double resonance (ENDOR) spectroscopy. ENDOR is important since it can yield information about the protonation state of a particular radical. Studies on single crystals are necessary in order to single out the individual components in full DNA, the spectrum of which is very complex. In fact, even the spectra of the individual bases are elaborate due to significant hydrogen bonding in the crystal structures. Thus, assignment of these spectra often requires simulations, assumptions of possible mechanisms, and/or other additional arguments.

Since some unknowns still exist as to which DNA radiation products are the most important, theoretical calculations may be able to play an important role. In particular, density functional theory (DFT) has been shown to yield very accurate

hyperfine coupling constants (HFCCs) at a reduced computational cost relative to other methods appropriate for the calculation of this property.^{14,15} Extensive studies on the other DNA bases, thymine and its derivatives,¹⁶ cytosine,¹⁷ and adenine,¹⁸ as well as radicals formed in the sugar moiety,¹⁹ have been performed with great success using DFT. Comparison of the calculated and the experimental HFCCs provides important information for identifying the radicals formed upon irradiation of the single crystals of each DNA base. Subsequent comparison of the spectra of these assigned radicals to the spectrum of full DNA allows for the identification of some of the main products of DNA radiation damage.

As previously mentioned, guanine is important to investigate since it has been proposed to be the main site of electron loss upon irradiation of DNA. Similar to adenine, guanine has been examined in a variety of crystalline environments. Studies of possible radical products in different environments provide a better understanding of how the environment affects which radicals are formed, important information when transferring results obtained from single crystals to full DNA. For example, detailed ESR/ENDOR studies on single crystals of guanine hydrobromide monohydrate²⁰ were used to render information about the importance of “bound” water to radical formation. On the other hand, the examination of 2'-deoxyguanosine 5'-monophosphate crystals²¹ supplied information about the influences of the sugar moiety and the phosphate group on radical formation.

In the present study, DFT is used to investigate the possible hydrogenated (net H• addition), dehydrogenated (net H• removal), and hydroxylated (net OH• addition) products formed upon irradiation of the DNA base guanine (Figure 1, I). The

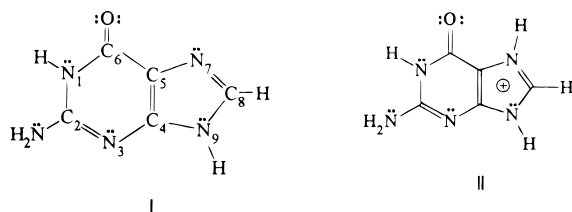


Figure 1. Molecular structure and atomic numbering of guanine (I) and N7-protonated guanine (II).

mechanisms resulting in such radical products will be the subject of papers to appear soon. The first step is to identify the important products. Experimental ESR/ENDOR studies have evolved around a variety of crystalline environments in which the parent guanine molecule is protonated at the N7 position (Figure 1, II). For example, Hole et al.²⁰ performed a study on guanosine hydrobromide monohydrate crystals in which the N7 position is protonated. Examination of protonated guanine model systems, such as the one studied by Hole et al., is important since in nonprotonated crystals the guanine cation is readily deprotonated even at low temperatures. Thus, investigation of the radical, thought to be predominantly formed in full DNA, namely the guanine cation, is extremely difficult in nonprotonated samples. However, in N7-protonated crystals, deprotonation primarily occurs at the N7 position after loss of an electron. The spectrum of this product is hence very similar to that assigned to the guanine cation observed in DNA.²² Due to the importance of the N7-protonated radicals, some of these have also been investigated in the current study where experimental data is available.

Theoretical Details

Becke's three-parameter exchange functional (B3)²³ in combination with Lee, Yang, and Parr's correlation functional (LYP)²⁴ and Pople's 6-31G(d,p) basis set²⁵ were used to perform geometry optimizations and frequency analyses. The zero-point energy was scaled according to the factor suggested by Bauschlicher and Partridge²⁶ (0.9804). Subsequent single-point calculations were performed at the B3LYP level with Pople's 6-311G(2df,p) basis set²⁵ to obtain relative energies, spin densities, and dipole moments of the global minima. These calculations were performed using Gaussian 94.²⁷ The hyperfine coupling constants were obtained with Perdew and Wang's nonlocal exchange (PW),²⁸ Perdew's nonlocal correlation functional (P86),²⁹ and Pople's 6-311G(2d,p) basis set²⁵ through the deMon program.³⁰ The units of gauss (G), which can be converted to megahertz (MHz) by a factor of 2.8025, are used throughout.

Many good reviews on the accurate calculation of HFCCs exist in the literature^{14,15} and, thus, the details of theoretical requirements and methodology will not be reviewed here. However, it should be noted that accurate isotropic HFCCs (A_{iso}) require both a good description of electron correlation and a well-defined basis set, whereas satisfactory anisotropic HFCCs (T_{ii}) can be obtained with almost any theoretical method and basis set provided the structure is qualitatively correct. Thus, comparison of anisotropic hyperfine tensors can be used as an accurate guide to identify radical sites even when less satisfactory agreement is obtained for the isotropic component. Full tensor components are obtained through the addition of the isotropic HFCC to each component of the anisotropic tensor (i.e., $A_{ii} = A_{\text{iso}} + T_{ii}$).

TABLE 1: Relative Energies of Guanine Radicals (kcal/mol)

radical	relative energy
IP	171.8
EA	-15.8
C8-hydrogenated	0
N7-hydrogenated	11.0
C4-hydrogenated	14.8
O6-hydrogenated	19.5
N3-hydrogenated	21.6
C5-hydrogenated	35.8
N9-dehydrogenated	0
N1-dehydrogenated	1.7
N2-dehydrogenated	1.9
C8-dehydrogenated	24.1
C8-hydroxylated	0
C4-hydroxylated	14.2
C5-hydroxylated	19.0

Results and Discussion

Guanine Anion and Cation. The adiabatic ionization potential (IP) and electron affinity (EA) of guanine are displayed in Table 1, along with the relative energies of other possible radiation products. The ionization potential was calculated to be 171.8 kcal/mol using DFT, which is in agreement with both the experimental value³¹ (179.3 kcal/mol) and the value obtained at the MP2/6-31+G(d) level of theory³² (176.6 kcal/mol). Unlike the ionization potential, the electron affinity has not been determined experimentally. In the present study, the EA was calculated to be -15.8 kcal/mol. This value is similar to that predicted from the vertical electron affinities through a best fit of the Koopman's EAs calculated using a combination of the HF method and the D95v//6-31G* basis sets (-16.7 kcal/mol).³²

Both the guanine anion and the guanine cation have been proposed to be formed upon irradiation of a variety of guanine crystals. The anion was reported in a study of the crystals of 2'-deoxyguanosine 5'-monophosphate.²¹ The spin density at C8 of the observed radical in 2'-deoxyguanosine 5'-monophosphate was determined to be 0.11. This spin density is different from those calculated in the present study, displayed in Table 2, which predicts over half of the spin to reside on C2 and smaller amounts to be located on N2 and C8. It should be noted that the C8 spin density, in particular, can be altered by the hydrogen-bonding environment at N7.²¹ In particular, the results presented within and the experimental results may differ since experimentally hydrogen bonding is evident which was not accounted for in the calculations. The geometry optimization of the anion indicated that this radical undergoes significant geometrical alterations upon radical formation. In particular, the pyrimidine (six-membered) ring is distorted at the C2 position and the amino group is located out of the plane. The amino group is also twisted such that one hydrogen is orientated directly perpendicular to the plane formed by the remainder of the guanine molecule and the other hydrogen is located at an angle of 104° with respect to it. This distortion leads to a localization of the spin density at the C2 (0.57) and the N2 (0.12) positions.

The experimental coupling constants attributed to the anion are displayed in Table 3. It can be seen that a significant C8-H isotropic coupling was observed (-3.0 G). This value is in good agreement with the calculated isotropic coupling (-2.5 G) displayed in Table 4. However, the calculated (-1.6, -0.1, 1.6 G) and experimental (-2.5, 0, 2.5 G) anisotropic tensors differ more than expected since this component can be calculated to a greater degree of accuracy than the isotropic contribution. In addition, the calculations indicate that a large N2-H isotropic coupling (31.9 G) would be observed due to the out of plane amino hydrogen.

TABLE 2: Calculated Spin Density Distributions in Guanine Radicals

radical	N1	C2	N2	N3	C4	C5	C6	O6	N7	C8	N9
anion		0.57	0.12							0.08	
C_s anion		0.51	0.07		0.20	0.10				0.08	
cation			0.10	0.21	0.17	0.29				0.28	
N3-hydrogenated	0.11	0.68									
C4-hydrogenated						0.48		0.16		0.23	0.12
C5-hydrogenated		0.32			0.44						
O6-hydrogenated					0.14		0.64	0.09			
C_s O6-hydrogenated					0.22		0.53			0.07	
N7-hydrogenated									0.17	0.61	0.08
C8-hydrogenated					0.13			0.10	0.51		0.11
N1-dehydrogenated	0.32			0.31				0.21		0.25	
N2-dehydrogenated		-0.11	0.37	0.35		0.28				0.19	
C8-dehydrogenated										0.82	
N9-dehydrogenated			0.08		0.19	0.16		0.13	0.14	0.23	
C4-hydroxylated						0.48		0.17		0.26	
C5-hydroxylated		0.25			0.44			0.10			
C8-hydroxylated					0.13			0.12	0.47		

TABLE 3: Experimental HFCCs (G) in Guanine Radicals

radical	molecule	atom	A_{iso}	T_{xx}	T_{yy}	T_{zz}
anion	2'-deoxyguanosine	C8-H	-3.0	-2.5	0.0	2.5
	5'-monophosphate ²¹					
cation	guanine:HCl:H ₂ O ³³	N2-H	4.3	-3.8	0.7	3.2
		N2-H	4.3	-3.8	0.7	3.2
		C8-H	5.2	-2.2	-0.2	2.3
	guanine:HCl:H ₂ O ³⁴	C8-H	-4.0	-2.0	-0.4	2.5
	guanosine 3'5'-cyclic monophosphate ³⁵	C8-H	-4.5	-2.7	-0.8	3.4
	guanine:HBr:H ₂ O ²⁰	C8-H	-4.6	-2.4	-0.4	2.8
N2-dehydrogenated	2'-deoxyguanosine	N2-H	-9.5	-6.9	-0.9	7.7
	5'-monophosphate ²¹	C8-H	-5.0	-2.5	-0.1	2.6
	3'5'-cyclic guanosine	N2-H	-9.5	-6.9	-1.0	7.9
	5'-monophosphate ²²	C8-H	-4.7	-2.4	-0.2	2.7
	2'-deoxyguanosine	N2-H	-9.6	-6.9	-0.9	7.8
	5'-monophosphate ³⁶	C8-H	-4.9	-2.6	-0.2	2.9
C5-hydrogenated	2'-deoxyguanosine	C5-H	54.0	-1.0	-0.5	1.7
	5'-monophosphate ²¹					
C8-hydrogenated	2'-deoxyguanosine	C8-H	39.3	-1.4	-0.8	2.1
	5'-monophosphate ²¹	C8-H	37.2	-1.4	-0.8	2.2
	2'-deoxyguanosine	C8-H (2)	37.8	-0.8	-0.5	1.4
	5'-monophosphate ³⁸					
C4-hydroxylated	3'5'-cyclic guanosine	C8-H	-6.7	-3.4	-0.2	3.6
	5'-monophosphate ²²					
unassigned	2'-deoxyguanosine	C8-H	-7.2	-3.7	-0.3	4.0
	5'-monophosphate ²¹	N-H	-3.4	-2.6	-0.5	2.9
		N-H	-3.0	-1.9	-0.5	2.4

TABLE 4: Calculated HFCCs in the Guanine Anion and Cation Radicals (G)

radical	atom	A_{iso}	T_{xx}	T_{yy}	T_{zz}
anion	N2-H	1.6	-2.1	-1.1	3.2
	N2-H	31.9	-1.8	-0.9	2.7
	C8-H	-2.5	-1.6	-0.1	1.6
	N9-H	-1.4	-0.9	-0.6	1.6
C_s anion	N1-H	-3.2	-2.8	-1.0	3.7
	N2-H	-2.5	-2.2	-1.0	3.2
	N2-H	-2.8	-2.4	-0.8	3.2
	C8-H	-3.5	-2.0	-0.2	2.2
	N9-H	-3.4	-3.0	-0.8	3.7
cation	N2-H	-2.7	-1.6	-1.0	2.6
	N2-H	-3.1	-2.5	-0.7	3.2
	C8-H	-8.2	-4.4	-0.6	5.0

Through comparison of the calculated and the experimental HFCCs of the guanine anion, it is difficult to conclude whether the anion was actually observed experimentally. Possibly the large N2-H coupling calculated in this work will aid in the identification of the anion in future studies. However, reorientation of the amino group may not be possible in the experiments due to hydrogen-bonding possibilities in the crystals not accounted for in the previously discussed calculations. In order

to account for the fact that hydrogen bonding may yield planar radicals in the experiments, the geometry of the anion was optimized in a fixed C_s symmetry. The radical obtained from this constrained optimization lies 17.9 kcal/mol higher in energy. A frequency analysis was not performed since several negative eigenvalues are expected with a constrained optimization corresponding to a saddle point on the potential energy surface. The HFCCs for this planar anion are located in Table 4 under the heading C_s anion. The results improve the agreement with experiment. However, it is very difficult to conclude through comparison of the experimental and theoretical results whether the anion is responsible for the observed spectra. The C8-H anisotropic HFCCs are in better agreement with experiment for the planar anion than the nonplanar form, but the results are still not as good as observed for other radicals when the size of the couplings is considered. In addition, couplings of equal magnitude or larger were calculated for the two amino hydrogens, the N1-H and the N9-H, which were not reported experimentally. In order to make a positive identification of the radical which yields the observed spectra, additional experimental studies would be useful to determine the magnitude

of the aforementioned couplings. Hole et al.²¹ noted that the spectra assigned to the guanine anion in their study could possibly be due to the O6-hydrogenated radical. This option will be discussed in more detail below.

The guanine cation was observed in single crystals of guanosine hydrochloride monohydrate,^{33,34} guanine hydrobromide monohydrate,²⁰ and guanosine 3',5'-cyclic monophosphate.³⁵ In crystals of guanosine hydrochloride or hydrobromide monohydrate, the parent guanine molecule is protonated at the N7 position. When this protonated molecule is oxidized, the N7-dehydrogenated radical is formed with respect to the initially protonated parent molecule. The net result is equivalent to the guanine cation and, thus, the net radical reported in all of the above experimental studies is the guanine cation. The C8 spin density distributions in the various crystalline environments discussed above ranged from 0.14 to 0.182, which is a much lower percentage than the value of 0.28 obtained from the present calculations (Table 2). In guanine:HCl:H₂O crystals, the N3 spin density was determined to be 0.28, which is in good agreement with the calculated value of 0.21. The N2 spin density ranged from 0.15 to 0.17 in the guanine:HCl:H₂O crystals and from 0.06 to 0.08 in guanine:HBr:H₂O, which are also in fair agreement with the calculated spin density at this position (0.10).

Unlike the guanine anion, the radical cation's geometry retains a planar conformation upon optimization. The calculated isotropic C8-H coupling (−8.2 G), along with the anisotropic component (largest tensor component 5.0 G), is larger in magnitude than the experimental results (average isotropic component and largest anisotropic tensor component are −4.6 and 2.8 G, respectively). In addition, two N2-H coupling tensors were extracted in one study of guanine hydrochloride monohydrate crystals.³³ Once again, the experimental and calculated couplings differ to a great extent. Thus, it is speculated that the guanine cation was probably not observed directly in these studies, but more likely a deprotonated radical is formed. The exact identity of the deprotonated cation is difficult to determine through the comparison of theoretical and experimental HFCCs at this stage. Further experimental and theoretical work would be advantageous in order to determine which radical is responsible for the observed spectrum.

Guanine Dehydrogenated Radicals. The relative energies and spin density distributions of the dehydrogenated radicals, or the net hydrogen removal radicals, are displayed in Tables 1 and 2, respectively. From the energetics, it can be seen that the N9-dehydrogenated radical is the lowest energy species, with the N1- and N2-dehydrogenated radicals lying 1.7 and 1.9 kcal/mol higher in energy, respectively. In full DNA samples, the hydrogen at the N9 position is replaced by a sugar group and, thus, the N1- and the N2-dehydrogenated radicals will be the lowest energy radicals. The C8-dehydrogenated radical was also investigated in the present study and was found to lie much higher in energy (24.1 kcal/mol) than the lowest energy radical in this class. The high energy of this radical is probably the reason that it has not been observed in any experimental studies on guanine crystals to date.

The only dehydrogenated radical generated from nonprotonated crystals for which experimental HFCCs exist is the N2-dehydrogenated radical. This radical has been observed in 2'-deoxyguanosine 5'-monophosphate^{21,36} and 3',5'-cyclic guanosine 5'-monophosphate.²² The C8 spin density distribution in all samples was determined to be approximately 0.17, a slightly smaller value than calculated in the present study (0.19). In addition, all experimental studies concluded that the N2 spin

TABLE 5: Calculated HFCCs in Dehydrogenated Radicals (G)

radical	atom	A_{iso}	T_{xx}	T_{yy}	T_{zz}
N1-dehydrogenated	N2-H	−1.6	−0.9	−0.6	1.5
	N2-H	−2.0	−1.6	−0.5	2.1
	C8-H	−7.4	−4.1	−0.4	4.5
N2-dehydrogenated	N2-H	−7.6	−6.6	−1.2	7.7
	C8-H	−6.0	−3.4	−0.3	3.7
C8-dehydrogenated	N9-H	−1.4	−3.1	−1.8	4.9
N9-dehydrogenated	N2-H	−2.1	−1.5	−0.9	2.4
	N2-H	−2.0	−2.2	−0.6	2.8
	C8-H	−6.6	−3.7	−0.7	4.4

density is 0.33, which agrees very well with the value obtained through the use of DFT (0.37). The N3 spin density (0.31) was determined in the study of 3'5'-cyclic guanosine 5'-monophosphate crystals²² and this result is also in agreement with the calculations (0.35). Thus, it can be concluded that the spin density distribution obtained from the optimized planar structure of the N2-dehydrogenated radical is well described through the level of theory employed in the present study.

The experimental couplings for the N2-dehydrogenated radical obtained in the various studies (Table 3) are remarkably similar. The C8-H coupling tensor consists of an average isotropic component of −4.9 G and an average anisotropic component of (−2.5, −0.2, 2.7 G). This is in only fair agreement with the calculated values ($A_{\text{iso}} = -6.0$ G; $T_{ii} = -3.4, -0.3, 3.7$ G). The remaining amino hydrogen was also observed in the experimental studies. An isotropic HFCC, averaged between the three studies, of −9.6 G was assigned to the N2 hydrogen, which again is larger in magnitude than the N2-H coupling obtained from the DFT calculations (−7.6 G). However, through comparison of the experimental (−6.9, −1.0, 7.8 G) and the calculated (−6.6, −1.2, 7.7 G) anisotropic N2-H coupling tensor, it can be concluded that the experimental assignment of this coupling to the hydrogen at N2 and the spectrum to the N2-dehydrogenated radical is correct.

From the DFT calculations, it is evident that both of the N1- and the N9-dehydrogenated radicals remain planar upon formation, with very slight distortions occurring primarily at the amino group. The spin density (Table 2) in both of these radicals was calculated to be distributed throughout the two molecular rings. The hyperfine coupling constants (Table 5) in these dehydrogenated radicals were also very similar and consist of a notable C8-H coupling (approximately −7 G) which has a considerable amount of anisotropy (largest component of the anisotropic tensor is approximately 4.5 G). In addition, small coupling tensors were calculated for both of the amino hydrogens. The optimized C8-dehydrogenated radical also exhibited slight distortions, mainly at C8. A large part of the spin density is localized on C8 (0.82), which is in turn responsible for the only coupling that would be observed for this radical. In particular, the N9-H has a small isotropic coupling (−1.4 G), but more importantly it has a significant anisotropic tensor (−3.1, −1.8, 4.9 G) which would aid in the experimental detection of this radical.

Guanine Hydrogenated Radicals. The relative energies, spin densities, and HFCCs for the possible hydrogenated radicals, or the radicals formed through net addition of a hydrogen atom, are displayed in Tables 1, 2, and 6, respectively. Six net hydrogen addition radicals are possible of which the C8-hydrogenated radical is the lowest in energy. The N7-, C4-, O6-, and N3-hydrogenated radicals are 11.0, 14.8, 19.5, and 21.6 kcal/mol higher in energy, respectively. The C5-hydrogenated radical is the highest energy hydrogenated radical lying 35.8 kcal/mol above the corresponding C8 adduct.

TABLE 6: Calculated HFCCs in Hydrogenated Guanine Radicals (G)

radical	atom	A_{iso}	T_{xx}	T_{yy}	T_{zz}
N3-hydrogenated	N1-H	-2.0	-3.1	-1.8	4.9
	N2-H	31.8	-1.5	-1.1	2.6
	N2-H	7.7	-2.3	-1.5	3.9
	C8-H	-1.7	-1.0	-0.1	1.2
C4-hydrogenated	N2-H	1.0	-0.3	-0.2	0.5
	C4-H	42.7	-0.9	-0.6	1.5
	C8-H	-7.1	-4.1	-0.7	4.7
	N9-H	-3.4	-3.3	-1.2	4.5
C5-hydrogenated	N2-H	-1.0	-1.5	-0.8	2.3
	N2-H	12.4	-1.4	-0.9	2.4
	C5-H	49.5	-0.7	-0.5	1.2
O6-hydrogenated	N1-H	7.1	-2.0	-1.9	3.9
	O6-H	-2.8	-3.9	-2.4	6.3
	C8-H	-2.7	-1.6	-0.1	1.7
C_s O6-hydrogenated	N1-H	-3.0	-2.6	-1.2	3.8
	N9-H	-1.9	-2.2	-2.2	4.4
	C8-H	-3.9	-2.3	-0.1	2.3
N7-hydrogenated	N7-H	11.3	-4.3	-2.3	6.6
	C8-H	25.1	-7.6	-1.1	8.7
C8-hydrogenated	N2-H	1.6	-0.8	-0.4	1.2
	N2-H	-0.3	-0.9	-0.4	1.3
	C8-H	36.9	-1.1	-0.7	1.8
	C8-H	37.2	-1.1	-0.7	1.8
	N9-H	-2.9	-2.6	-0.9	3.5

Considering that only the C8 and the C5 radicals have been observed in the experimental studies, factors other than the thermodynamics considered here must be affecting the formation of the C5-hydrogenated radical.

The radical formed through net addition of hydrogen to the C5 position was observed in the crystals of 2'-deoxyguanosine 5'-monophosphate.²¹ The calculated geometry for this radical indicates that great geometrical distortions occur upon formation. In particular, the pyrimidine and imidazole (five-membered) rings remain planar but are tilted about the C4C5 bond toward each other. Colson and Sevilla,³⁷ who described the geometry as a "butterfly" conformation, have previously observed this distortion. Colson and Sevilla³⁷ also discussed another conformer, much higher in energy, in which the rings are tilted to opposite sides of the C4C5 bond. The C4-hydrogenated radical has not been assigned in any experimental study to date but was investigated in the present study. The calculations indicate that the geometry of this radical also adopts the aforementioned butterfly conformation. Similar geometries were obtained in a previous study for the adenine C4 and C5 hydrogen addition radicals.¹⁸ The dihedral angles which describe this distortion are displayed in Table 7. The distortion for both radicals is very similar.

The spin density in the C5-hydrogenated radical was calculated to reside primarily on C4 (0.44) and C2 (0.32). The experimental study indicated that the hydrogen that has been added to the guanine C5 position has a very large isotropic coupling (54.0 G) and a very small anisotropic coupling tensor (-1.0, -0.7, 1.7 G). The anisotropic coupling tensor is in good agreement with that calculated using DFT (-0.7, -0.5, 1.2 G). In addition, the calculated isotropic C5-H coupling (49.5 G) also supports the experimental assignment of the observed spectrum to the C5-hydrogenated radical. The calculations show that a hydrogen added to the C4 position in the corresponding C4-hydrogenated radical exhibits a slightly smaller, yet significant, isotropic coupling (42.7 G). The difference between the C4- and the C5-hydrogenated radicals is the significant isotropic coupling (12.4 G) calculated for one of the amino hydrogens in the C5-hydrogenated radical. This coupling might be useful for the clear identification of the C5-hydrogenated radical in future experimental studies.

The C8-hydrogenated radical was observed in two different studies on 2'-deoxyguanosine 5'-monophosphate,^{21,38} and the results are presented in Table 3. In the earliest study,³⁸ the spin density was determined to reside mainly on the nitrogen atoms; in particular, a spin density of 0.43 was assigned to N7. This is in agreement with the calculations which indicate that the spin density on N7 and N9 is 0.51 and 0.11, respectively, although there also exists considerable spin on C4 (0.13) and O6 (0.10). It was determined³⁸ that the two C8 hydrogens have equivalent isotropic couplings of 37.8 G. In a more recent study,²¹ the C8 hydrogens were assigned different isotropic couplings, namely 39.3 and 37.2 G. In the present study, the C8-hydrogenated radical was optimized to a mostly planar structure, with the exception of the amino group, and two slightly different couplings were obtained for the C8 hydrogens (37.2 and 36.9 G). It is noted that difficulties in accurately describing the puckering in radicals formed through addition of a hydrogen atom to the outside of the molecular ring have previously been observed for both thymine¹⁶ and adenine.¹⁸ Thus, from comparison of these previous calculations and the results presented within, it can be speculated that the difference between the two C8-H couplings is probably larger than obtained through the DFT calculations and that the later experimental results are more accurate. In addition, comparison of the anisotropic couplings obtained in both experimental studies to those obtained from the present calculations indicates that the observed radical can confidently be assigned to that formed through net hydrogen atom addition to the C8 position in guanine.

In addition to the extensive geometrical alterations observed for the C4- and C5-hydrogenated radicals, other hydrogen addition radicals also undergo differing degrees of distortion. The N3-hydrogenated product was calculated to exhibit significant puckering in the pyrimidine ring, in particular at the C2 position with the amino group twisted such that one hydrogen is above the plane formed by the rest of the molecule and the second hydrogen below the plane. This is a similar structure to that which was previously discussed for the radical anion. This distortion in the N3-hydrogenated radical results in a large percentage of the spin density to be localized on C2 (0.68) and N1 (0.11). Distortion in the N7-hydrogenated radical occurs in both the five- and six-membered rings. The C8, N7, and O6 positions are in this case all located out of the molecular plane which leads to a localization of the spin in the imidazole ring (Table 2). Neither of these net hydrogen atom addition radicals is believed to have been observed in experimental studies. The calculated HFCCs are displayed in Table 6 to aid in the future detection of these radicals. It should be noted that the N3 and N7 radicals may not be puckered in experimental crystals where hydrogen-bonding effects might be important. Further studies on the C_s structure of these radicals were not performed due to lack of experimental HFCCs in order to compare with the theoretical results and, thus, determine which theoretical model is more adequate.

The substituents in the O6-hydrogenated radical are greatly affected by radical formation. The O6 position is displaced out of the molecular plane with a dihedral angle with respect to C4 of 33.2°. In addition, the relative location of the amino hydrogens is affected by this distortion. This distortion is probably due to the large amount of spin density calculated to be located on C6 (0.64). The hydrogen at N1 is also slightly out of the molecular plane in this radical. Hole et al.²¹ determined that the O6-hydrogenated radical was unlikely to give rise to a C8 spin density of 0.11 and a resulting C8-H

TABLE 7: Dihedral Angles (deg) Which Define the Distortion in the C4 and C5 Hydrogen and Hydroxyl Radical Addition Products

	C4-hydrogenated	C5-hydrogenated	C4-hydroxylated	C5-hydroxylated
N3C5C4N7	129.5	-160.7	131.4	-159.3
N3C5C4C6	-39.4	-34.8	-37.9	-33.8
N9C5C4N7	6.9	12.1	10.9	12.6
N9C5C4C6	-162.0	138.0	-158.3	138.1

coupling ($A_{\text{iso}} = -3.0$ G; $T_{ii} = -2.5, 0, 2.5$ G) in 2'-deoxyguanosine 5'-monophosphate, but rather these properties are the result of the guanine anion. As previously discussed, comparison of the calculated and experimental couplings for the anion leads to some concern. However, the couplings for C8-H in the O6-hydrogenated radical are only in fair agreement with the experimental results obtained for the "anion" ($A_{\text{iso}} = -2.7$ G; $T_{ii} = -1.6, -0.1, 1.7$ G) and the spin density on C8 is extremely small. In addition, a larger N1-H isotropic coupling (7.1 G) was calculated, but not observed experimentally. It seems unlikely that this coupling, which is larger than that of C8-H, would go undetected in the experimental spectrum.

As previously discussed for the guanine anion, crystal interactions may lead to a planar O6-hydrogenated radical experimentally rather than the puckered form discussed to this point. If the geometry of the O6-hydrogenated radical is constrained to a C_s symmetry, the resulting radical lies only 3.8 kcal/mol higher in energy than the greatly distorted radical. The HFCCs are displayed in Table 6 (C_s O6-hydrogenated). As expected, the N1-H HFCC in the planar radical is much smaller in magnitude than that previously discussed for the nonplanar form. In addition, the C8-H HFCCs are larger in magnitude than those exhibited in the nonplanar radical. In particular, the C8-H anisotropic couplings in the planar O6-hydrogenated radical (-2.3, -0.1, 2.3 G) are in very good agreement with the anisotropic couplings assigned experimentally to the guanine anion (-2.5, 0.0, 2.5 G). In addition, the calculated C8 spin density (0.07) is not far from the spin density predicted experimentally (0.11) for the observed radical. Thus, it is possible that the spectrum, which was concluded to arise from the guanine anion experimentally, actually arises from the anion protonated at the O6 position. As previously mentioned, more experimental work, such as the determination of the N1-H HFCCs or searching for the O6-H coupling through ENDOR spectroscopy, would be beneficial for the full assignment of the observed radical. The calculations indicate that the planar anion and O6-hydrogenated radicals can be distinguished through the characterization of the amino hydrogen couplings. The amino hydrogens yield significant couplings in the anion that are not observed for the O6-hydrogenated radical.

Guanine Hydroxylated Radicals. Three radicals can be formed through the net addition of a hydroxyl radical to either the C4, C5, or C8 positions in guanine. The relative energies of these radiation products (Table 1) indicate that the C8-hydroxylated radical is the lowest in energy with the corresponding C4 and C5 radicals lying 14.2 and 19.0 kcal/mol higher in energy, respectively. This is identical to the relative energies calculated for the corresponding hydrogenated radicals. The only hydroxylated product that has been observed in experimental studies on neutral guanine crystals is the C4 hydroxylated radical. However, the other two possible products considered in the present section have been observed in various N7-protonated guanine derivatives.

The spin density distributions in the nonprotonated hydroxylated radicals (Table 2) indicate that in all of the radicals, close to half of the spin density is located on a neighboring center, in particular on C5 (0.48), C4 (0.44), and N7 (0.47) in the C4-,

TABLE 8: Calculated HFCCs in Hydroxylated Radicals (G)

radical	atom	A_{iso}	T_{xx}	T_{yy}	T_{zz}
C4-hydroxylated	C8-H	-7.8	-4.5	-0.7	5.1
	N9-H	-2.0	-2.5	-1.0	3.6
C5-hydroxylated	N2-H	7.6	-1.5	-0.8	2.4
	N7-H	-1.0	-1.1	-0.9	2.0
C8-hydroxylated	C8-H	-2.5	-1.5	-0.5	2.0
	C8-H	23.4	-1.0	-0.5	1.5
	N9-H	-2.4	-2.1	-0.8	2.9

C5-, and C8-hydroxylated radicals, respectively. Both the C4- and C5-hydroxylated radicals adopt the butterfly conformation previously discussed for the guanine C4- and C5-hydrogenated radicals, as well as that discussed by Colson and Sevilla³⁷ and calculated in adenine radicals.¹⁸ The dihedral angles defining this butterfly conformation are displayed in Table 7 and compared to those angles obtained for the corresponding hydrogenated radicals. Most of the angles in the hydrogenated versus hydroxylated adducts differ by no more than 2°. The largest difference between the two sets of angles occurs for the N9C5C4N7 and N9C5C4C6 angles which differ by 4° in the hydroxylated radical relative to the hydrogen addition product. Significant isotropic couplings were calculated for C8-H (-7.8 G) or N2-H (7.6 G) in the C4- and C5-hydroxylated radicals, respectively.

The geometry of the C8-hydroxylated radical, on the other hand, is not significantly different from the parent molecule. The amino group in the C8-hydroxylated radical is distorted more than observed for the parent molecule. The hydrogen and the hydroxyl group at the C8 position are orientated such that they are displaced equally on opposite sides of the molecular plane. The displacement of the C8-hydrogen from the molecular plane by the hydroxyl group leads to a substantial C8-H isotropic coupling (23.4 G). The full hyperfine coupling tensors for these hydroxylated radicals appear in Table 8.

The spectrum of the C4-hydroxylated radical was recorded in crystals of guanosine monophosphate.²² It was determined that the observed radical possesses a C8 spin density of approximately 0.25. The calculated results for the nonprotonated C4-hydroxylated radical indicate that a spin density of 0.26 is located at C8, which is in excellent agreement with experiment. The only coupling which was determined experimentally for this radical was for C8-H, whose full coupling tensor is (-10.1, -6.9, -3.1 G). The calculated full tensor for the proposed radical is (-12.3, -8.5, -2.7 G), which is in only fair agreement with experiment when the individual components of the coupling tensor are considered.

Of the radicals investigated in the present study, the only couplings that match the experimental C8-H isotropic (-6.7 G) and anisotropic results (-3.4, -0.2, 3.6 G) arise from the nonprotonated N2-dehydrogenated radical. The C8-H calculated tensor in this radical is composed of a -6.0 G isotropic component and an anisotropic tensor of (-3.4, -0.3, 3.7 G). This radical also possesses a large N2-H coupling (-7.6 G), which was not identified experimentally. More studies would be extremely useful for the full identification of this radical.

Experimentally Unassigned Guanine Radical. In a study of 2'-deoxyguanosine 5'-monophosphate, Hole et al.²¹ observed

TABLE 9: Experimental HFCCs (G) of N7-Protonated Guanine Radicals

radical	molecule	atom	A_{iso}	T_{xx}	T_{yy}	T_{zz}
O6-hydrogenated	guanine:HCl:H ₂ O ³⁴	N1-H	-4.2	-2.5	-0.5	3.0
		C8-H	-7.5	-4.3	0.5	3.8
		C8-H	-8.1	-4.0	-0.3	4.3
	guanosine 5'-monophosphate ⁴⁰	N1-H	-3.7	-2.6	-0.6	3.2
		O6-H	0.4	-1.6	0.1	1.5
		N7-H	-3.3	-1.6	-1.0	2.6
	guanine:HCl:2H ₂ O ⁴¹	C8-H	-7.2	-3.5	-0.4	3.9
		N1-H	-2.2	-1.7	-0.1	1.7
		N7-H	-1.7	-1.7	-0.8	2.5
		C8-H	-7.7	-4.7	0.6	4.1
		N1-H	-4.1	-2.9	-0.6	3.4
		N7-H	-3.5	-2.2	-0.7	2.9
		C8-H	-7.6	-3.8	-0.4	4.2
		N1-H	-3.5	-2.5	-0.5	3.0
		N7-H	-3.1	-1.8	-0.9	2.7
		C8-H	-7.8	-4.1	-0.2	4.3
		N1-H	-3.2	-2.4	-0.6	3.0
		N7-H	-2.9	-1.6	-0.9	2.5
		C8-H	-8.3	-3.6	0.0	4.7
		N1-H	-3.2	-2.4	-0.5	2.9
		N7-H	-2.8	-1.6	-0.9	2.4
		C8-H	-8.1	-4.0	-0.6	4.5
C8-hydrogenated	guanine:HCl:H ₂ O ³⁹	C8-H	46			
		C8-H	25.8	-1.6	-0.3	1.7
		N7-H	-8.3	-6.6	-0.6	7.3
	guanosine 5'-monophosphate ⁴⁰	C8-H	36.5	-1.4	-0.7	2.1
		C8-H	33.1	-1.4	-0.8	2.1
		N7-H	-8.5	-6.6	-1.6	8.2
	guanine:HCl:2H ₂ O ⁴¹	C8-H	35.3	-1.3	0.0	2.1
		C8-H	38.2	-1.3	-0.9	2.1
		N7-H	-9.0	-6.9	-1.5	8.4
		N9-H	-3.0	-2.4	-0.7	3.1
		N7-H	-8.6	-7.2	-1.6	8.5
		N9-H	-3.2	-2.6	-0.8	3.0
N9-dehydrogenated	guanine:HCl:H ₂ O ³⁹	N7-H	-5.0	-3.6	-1.4	5.0
		N2-H	-2.2	-1.8	-0.3	2.1
		N2-H	-2.1	-1.4	-0.6	1.9
	guanine:HCl:2H ₂ O ⁴¹	N2-H	-2.0	-1.3	-0.5	1.8
		N2-H	-2.2	-1.5	-0.4	2.0
		N7-H	-5.4	-3.7	-1.3	5.1
C5-hydroxylated	guanine:HBr:H ₂ O ²⁰	N2-H	-4.0	-2.9	-0.6	3.5
		N2-H	-3.5	-2.2	-0.4	2.5
		N7-H	-3.2	-2.4	-1.0	3.4
		C8-H	-3.7	-1.9	-0.5	2.4
C8-hydroxylated	guanine:HCl:2H ₂ O ⁴¹	N7-H	-8.5	-6.5	-1.5	8.0
		C8-H	20.2	-1.1	-0.6	1.6
		N9-H	-2.2	-1.8	-0.7	2.5
ring-opened	guanine:HBr:H ₂ O ²⁰	C8-H	-4.9	-2.6	0.1	2.4

a spectrum that was unassigned to a particular species, although many possible radicals were discussed. The spectrum of the unassigned radical was determined to consist of a C8-H coupling ($A_{\text{iso}} = -7.2$ G, $T_{ii} = -3.7, -0.3, 4.0$ G) and two couplings due to hydrogens attached to nitrogen atoms. One N-H coupling possesses an isotropic component of -3.4 G and significant anisotropy ($-2.6, -0.5, 2.9$ G). This coupling was proposed to be due to either the hydrogen attached to N1 or an amino hydrogen. The second N-H coupling was suggested to arise from a hydrogen at N2 or N3 or alternatively from a hydrogen involved in hydrogen bonding to N7. This hydrogen has a similar isotropic component to the first (-3.0 G) but a slightly smaller anisotropic tensor ($-1.9, -0.5, 2.4$ G).

Two deprotonated radicals were suggested to possibly give rise to the unassigned spectrum, namely those formed via removal of a hydrogen from N1 or N2. Comparison of the experimental couplings (Table 3) and those calculated for the N2-dehydrogenated radical in the present study (Table 5) indicates that this radical is unlikely to be responsible for the observed spectrum. This can be seen since only one N-H

coupling was calculated for this radical which furthermore is significantly different from those discussed for the unidentified radical. The calculated couplings for the N1-dehydrogenated radical (Table 5) match those determined from the unassigned spectrum more closely, although the anisotropic couplings disagree more than expected for this component of the HFCC. It is interesting to note that the calculated anisotropic couplings for the N9-dehydrogenated radical are in excellent agreement with those of the unassigned radical. However, this radical is not expected in guanosine since a sugar group replaces the hydrogen at the N9 position in guanine.

Hole et al.²¹ also noted that the unassigned spectrum could be due to an O6-hydrogenated radical that is protonated at the N7 position. The calculated results for this radical have yet to be discussed in the present paper, but the calculations (Table 12) yield quite different HFCCs than those obtained experimentally for the unidentified radical for both the planar and nonplanar calculated geometries. The guanine cation was also discussed by Hole et al. as having a spectrum similar to that recorded, but unassigned, experimentally. The present calculations on the guanine cation (Table 4) support the hypothesis

TABLE 10: Relative Energies of N7-Protonated Guanine Radicals (kcal/mol)

radical	relative energy
C8-hydrogenated	0
O6-hydrogenated	18.8
C8-hydroxylated	0
C5-hydroxylated	20.5
ring-opened	28.8
N9-dehydrogenated	0

that the unassigned spectrum is similar to the guanine cation. The calculated N–H anisotropic couplings are in remarkable agreement with those obtained experimentally, whereas the calculated C8–H anisotropic coupling is slightly larger than the recorded value. The guanine cation was not seriously considered to be responsible for the observed spectrum since it is unlikely that this radical would be observed at 200 K.

In their study, Hole et al.²¹ commented on the similarity of the unassigned spectra to that obtained for both the guanine anion and guanine cation. In particular, they discussed the mandatory care required when interpreting the resonance patterns of the irradiated DNA bases, even for those spectra obtained from the sophisticated ENDOR technique. The calculations support these statements since many of the calculated HFCCs for the radiation products are very similar. Thus, even through the use of high-level calculations, interpretation of the observed spectra is very difficult. This example illustrates the great difficulties associated with the determination of DNA radiation products, even when the problem is reduced to examining the individual bases.

Guanine N7-Protonated Radicals. As previously discussed, it is very important to study the DNA radiation products in a variety of crystalline environments in order to better understand the differences when transferring results from single-crystal models to full DNA. In addition, since the guanine cation has been proposed to be one of the main radicals formed upon irradiation of full DNA samples and the cation is deprotonated even at low temperatures in nonprotonated crystal samples, it is important to study crystals of the N7-protonated parent molecules where the net guanine radical cation is readily formed. Thus, the present study investigates the HFCCs in N7-protonated guanine radicals for which experimental data (Table 9) exists.

The calculated relative energies, the spin density distributions, and the HFCCs of the N7-protonated radicals examined in this study are presented in Tables 10, 11, and 12, respectively. Two hydrogenated radicals were investigated, namely the C8 and O6 adducts. The relative energy of the two hydrogenated species indicates that the C8 hydrogen addition radical lies 18.8 kcal/mol below the corresponding O6 radical. This energy difference is very close to that previously observed (19.5 kcal/mol) for the nonprotonated species.

The C8-hydrogenated radical protonated at the N7 position was observed in studies on crystals of guanine hydrochloride monohydrate,³⁹ guanosine 5'-monophosphate,⁴⁰ guanine hydrochloride dihydrate,⁴¹ and guanine hydrobromide monohydrate.²⁰ The average spin density distribution observed in the various studies indicates that the spin density on N7 and N9 is approximately 0.31 and 0.11, respectively. The calculated results (Table 11) indicate that N7 and N9 have a respective spin density distribution of 0.32 and 0.10, in excellent agreement with experiment. In addition, the calculations indicate that significant spin also resides on C5 (0.31) and O6 (0.17). A coupling assigned to the hydrogen attached to the N7 position was present in all experimental studies which consists of an average -8.6 G isotropic component and a notable anisotropic

tensor ($-6.8, -1.3, 8.1$ G). This is in very nice agreement with the HFCC calculated for N7–H in the protonated C8-hydrogenated radical ($A_{\text{iso}} = -8.1$ G; $T_{ii} = -6.5, -1.8, 8.3$ G). In two studies,^{20,41} a coupling tensor for the N9–H was observed ($A_{\text{iso}} = -3.1$ G; $T_{ii} = -2.5, -0.8, 3.1$ G). Once again, close agreement is obtained between experiment and calculations where the calculations yield $A_{\text{iso}} = -3.0$ G and $T_{ii} = -2.5, -0.9, 3.4$ G.

The anisotropic C8–H couplings in all of the experimental studies were virtually identical, on average ($-1.4, -0.7, 2.0$ G). The calculated anisotropic C8–H tensor component ($-1.1, -0.7, 1.7$ G) is in good agreement with experiment. In contrast, the two isotropic C8–H couplings vary between crystalline environments as observed from the experimental results presented in Table 9. In some studies the difference between the two couplings is great³⁹ (approximately 20 G), while in other studies the difference is much smaller^{40,41} (3 G). The couplings in the two later studies may be regarded as more reliable since the complete coupling tensors were determined using sophisticated ENDOR spectroscopy, whereas the couplings which deviated by 20 G were determined only through the use of ESR. It should be noted, however, that differences in these couplings may also arise due to the crystalline environment, temperature, or different time scales in the experiments. The calculations indicate that the two C8 hydrogens have identical couplings which are much smaller (29.1 G) than those observed in any of the ENDOR experiments (approximately 34 and 37 G). The problem of calculating couplings which are smaller than those observed experimentally has previously been encountered for similar radicals in both thymine¹⁶ and adenine.¹⁸ However, due to the good agreement between theory and experiment for the spin density distribution and all of the couplings besides the isotropic C8–H component, it can be concluded that the calculations support the assignment of the protonated C8-hydrogenated radical.

The second N7-protonated, hydrogenated radical observed in the experimental studies is the O6 species. This radical was observed in studies on crystals of guanine hydrochloride monohydrate,³⁴ guanosine 5'-monophosphate,⁴⁰ guanine hydrochloride dihydrate,⁴¹ and guanine hydrobromide monohydrate.²⁰ Theoretically, the geometry was calculated to exhibit distortions in which the oxygen at C6 is located slightly out of the molecular plane forming a dihedral angle with C4 of 175.5° . The hydrogen attached to O6 is located out of the molecular plane at a dihedral angle with respect to C5 of 111.5° . The position of this hydrogen leads to a large isotropic O6–H HFCC, which is not observed experimentally, as to be discussed. The experimental and calculated couplings for this radical are displayed in Tables 9 and 12, respectively. The data in the two tables are quite different. The calculated couplings for the hydrogen at O6 (22.0 G) and C8 (-11.0 G) are extremely large, whereas the corresponding experimental couplings are small. Not even the anisotropic couplings are in fair agreement. In addition to the HFCCs, the experimental spin density was determined to reside (on average) on C8 (0.27), N1 (0.15), and N7 (0.11), but the calculated spin density (Table 11) reflects no similarities to this distribution. Thus, it seems unlikely that the N7-protonated O6 hydrogen addition radical led to the spectra observed in any of these studies.

Since hydrogen-bonding interactions in the crystals may force the geometry of the molecule to remain planar, additional calculations were performed in order to investigate the planar structure of the N7-protonated O6-hydrogenated radical. Through a complete geometry optimization, a planar structure was

TABLE 11: Calculated Spin Density Distributions in N7-Protonated Guanine Radicals

radical	N1	C2	N2	N3	C4	C5	C6	O6	N7	C8	N9
C8-hydrogenated						0.31		0.17	0.32		0.10
O6-hydrogenated	0.10				0.12		0.40			0.38	
C _s O6-hydrogenated	0.07						0.32		0.08	0.46	
C8-hydroxylated						0.33		0.18	0.30		
C5-hydroxylated		0.12			0.37					0.29	
ring-opened					-0.13	0.43				0.13	0.54
N9-dehydrogenated			0.13	0.23		0.32		0.18	0.10		

TABLE 12: HFCCs in Various Guanine N7-Protonated Cation Radicals (G)

radical	atom	A _{iso}	T _{XX}	T _{YY}	T _{ZZ}
O6-hydrogenated	O6-H	22.0	-1.5	-1.2	2.7
	N7-H	-2.4	-1.5	-1.2	2.7
	C8-H	-11.0	-6.2	0.3	5.9
C _s O6-hydrogenated	N1-H	-2.6	-2.2	-0.9	3.1
	O6-H	-1.5	-1.5	-1.5	2.9
	N7-H	-3.2	-2.3	-1.3	3.6
	C8-H	-12.8	-7.2	0.4	6.8
C8-hydrogenated	N2-H	-1.3	-0.9	-0.5	1.4
	N2-H	-1.6	-1.1	-0.4	1.5
	N7-H	-8.1	-6.5	-1.8	8.3
	C8-H	29.1	-1.1	-0.7	1.7
N9-dehydrogenated	C8-H	29.1	-1.1	-0.6	1.7
	N9-H	-3.0	-2.5	-0.9	3.4
	N2-H	-3.4	-2.1	-1.1	3.2
	N2-H	-3.8	-3.1	-0.8	3.9
C5-hydroxylated	N7-H	-2.8	-2.2	-1.1	3.3
	C8-H	-2.9	-1.7	-0.6	2.3
	N2-H	-2.5	-1.7	-0.9	2.7
	N2-H	-2.7	-2.4	-0.6	3.0
C8-hydroxylated	N7-H	-1.5	-1.5	-0.9	2.5
	C8-H	-9.1	-5.0	-0.2	5.2
	N7-H	-7.0	-5.9	-1.7	7.6
	C8-H	17.5	-0.9	-0.5	1.4
ring-opened	N9-H	-2.1	-1.8	-0.8	2.6
	N1-H	-1.3	-1.0	-0.5	1.5
	N7-H	-2.7	-1.3	0.1	1.3
	C8-H	-4.8	-2.5	-0.5	3.0
	O8-H	-1.0	-1.7	-1.0	2.7
	N9-H	-10.6	-9.3	-1.8	11.1

obtained which possesses one imaginary frequency indicating that this molecule is a transition state rather than a ground state molecule. However, since there is reason to believe the experimental geometry remains in a planar arrangement and the planar radical lies only 1.7 kcal/mol higher in energy than the nonplanar counterpart, the HFCCs were calculated for this molecule. The calculated HFCCs are displayed in Table 12 (C_s O6-hydrogenated). Agreement can be considered to be improved over the calculated results for the nonplanar O6-hydrogenated geometry since the calculations on the planar geometry yield only a small O6-H coupling which is expected experimentally. A N1-H coupling was also obtained which was not calculated for the nonplanar radical. In addition, the spin densities for the planar radical more closely match those obtained experimentally. However, even using a planar geometry, the spin density distribution is not in great agreement with experiment and the HFCCs obtained from experiment and theory do not agree. In particular, the C8-H isotropic and anisotropic HFCCs obtained from the calculations are far too large relative to those obtained in the experimental study.

The possibility that the observed radical is the nonprotonated O6-hydrogenated radical can be eliminated through the examination of the calculated couplings in this radical (Table 6). In particular, the C8-H HFCCs for both the planar and the nonplanar O6-hydrogenated radical are different from those assigned to the N7-protonated O6-hydrogenated radical. Also, clear couplings were observed experimentally for the N7

TABLE 13: Variation in the Planar, N7-Protonated O6-Hydrogenated Radical's C8-H and N7-H Couplings (G) with Respect to the N7-H Bond Length (Å)

bond length	C8-H				N7-H			
	A _{iso}	T _{XX}	T _{YY}	T _{ZZ}	A _{iso}	T _{XX}	T _{YY}	T _{ZZ}
0.908	-13.1	-7.3	0.4	6.9	-3.1	-2.9	-1.1	4.0
1.008 ^a	-12.8	-7.2	0.4	6.8	-3.2	-2.3	-1.3	3.6
1.108	-12.8	-7.1	0.4	6.7	-3.2	-1.9	-1.4	3.3
1.208	-12.6	-7.0	0.4	6.6	-3.5	-1.6	-1.4	3.0
1.308	-12.4	-6.9	0.4	6.5	-4.0	-1.4	-1.3	2.7
unprotonated ^b	-3.9	-2.3	-0.1	2.3				
experimental ^c	-7.8	-4.0	-0.1	4.2	-2.9	-1.8	-0.9	2.6

^a The optimized bond length for the planar N7-protonated O6-hydrogenated radical. ^b Results for the C_s O6-hydrogenated radical which is not protonated at N7. ^c The experimental value was obtained as an average of the results presented in Table 9.

hydrogen. In order to ensure that differences in the calculated and experimental C8-H couplings for the N7-protonated O6-hydrogenated radical do not arise due to differences in the hydrogen-bonding environment at N7, a series of calculations were performed where the N7-H bond length was varied. The results for the C8-H and N7-H HFCCs are displayed in Table 13. The N1 and O6 hydrogen couplings did not change with variations in the N7-H bond length and thus are not included in the table. From the results of this bond length variation study, it can be seen that the protonated O6-hydrogenated radical's C8-H couplings do not change substantially with the N7-H bond length. On the contrary, the N7-H anisotropic couplings show a decrease in magnitude with an increase in bond length. It is noted that a great difference is observed for the C8-H couplings in the planar protonated and nonprotonated radicals. However, neither of these couplings match those observed experimentally which were assigned to the protonated O6-hydrogenated radical.

A possible explanation of the observed spectrum can be obtained through examination of the average of the planar protonated and planar nonprotonated O6-hydrogenated radical's HFCCs. The average C8-H HFCC obtained for the protonated and nonprotonated radicals consists of an isotropic component of -8.4 G and an anisotropic tensor of (-4.8, 0.3, 4.6) G. This is in good agreement with the experimental C8-H coupling (A_{iso} = -7.8 G; T_{ii} = -4.0, -0.1, 4.2 G). The average calculated N1-H couplings (A_{iso} = -2.8 G; T_{ii} = -2.4, -1.1, 3.5 G) is also in agreement with the N1-H coupling assigned experimentally (A_{iso} = -3.4 G; T_{ii} = -2.4, -0.5, 2.9 G). In addition, any discrepancies between the experimental and calculated N7-H couplings can be explained in terms of differences in the N7-H bond length. From Table 13 and recalling that it is possible to calculate the anisotropic component to a greater degree of accuracy than the isotropic HFCC, it is evident that the experimental N7-H HFCCs are in better agreement with the calculations performed at longer bond lengths than that obtained through the optimizations. Thus, a possible explanation for the observed spectra is that an averaging is being recorded where some of the O6-hydrogenated radicals are protonated at the N7 position and some exist as nonprotonated.

TABLE 14: Variation in the N7–H and C8–H HFCCs (G) for the N7-Protonated N9-Dehydrogenated Radical with Respect to the N7–H Bond Length (Å)

bond length	C8–H				N7–H			
	A_{iso}	T_{XX}	T_{YY}	T_{ZZ}	A_{iso}	T_{XX}	T_{YY}	T_{ZZ}
0.908	–2.8	–1.7	–0.6	2.3	–2.8	–2.7	–0.9	3.6
1.008 ^a	–2.9	–1.7	–0.6	2.3	–2.8	–2.2	–1.1	3.3
1.108	–3.0	–1.8	–0.6	2.4	–2.9	–1.9	–1.2	3.1
1.208	–3.0	–1.8	–0.6	2.4	–3.3	–1.6	–1.3	2.6
1.308	–3.1	–1.8	–0.6	2.5	–3.8	–1.4	–1.3	2.6
1.408	–3.2	–1.9	–0.6	2.5	–4.7	–1.2	–1.2	2.4
1.508	–3.3	–2.0	–0.6	2.6	–6.1	–1.1	–1.0	2.2
unprotonated experimental ^b	–6.6	–3.7	–0.7	4.4	–5.2	–3.7	–1.4	5.1

^a The optimized bond length for planar N7-protonated N9-dehydrogenated radical. ^b The experimental value was obtained as an average of the results presented in Table 9.

nated radicals. The similarity between the averaged couplings and those left unassigned in 2'-deoxyguanosine 5'-monophosphate previously discussed in this paper is noted. This explanation may also account for the unassigned radical.

Unlike the spin density calculated for the planar and nonplanar N7-protonated O6-hydrogenated radical, the guanine cation is the only radical which has two calculated nitrogen spin densities of similar magnitude to those observed experimentally for the O6-hydrogenated radical cation. In particular, the calculated cation (0.28) and experimental O6-hydrogenated (0.27) C8 spin densities are in remarkable agreement. In addition, the calculated N2 (0.10) and N3 (0.21) spin density distributions for the cation are in agreement with the values obtained experimentally for the O6-hydrogenated radical which were assigned to N7 (0.11) and N1 (0.15), respectively. Examination of the full tensor components of the assigned couplings supports the speculation that the observed radical is possibly the guanine cation. For example, the (average) experimental (–11.9, –8.0, –3.5 G) and calculated (–12.6, –8.8, –3.2 G) full tensor C8–H couplings are in excellent agreement. In addition, the experimentally assigned N1 (–5.9, –3.9, –0.6 G) and N7 (–4.8, –3.8, –0.3 G) tensors in the O6-hydrogenated radical are in excellent agreement with those calculated for the two N2 hydrogens, (–5.6, –3.8, 0.1 G) and (–4.3, –3.7, –0.1 G), respectively. Hence, the experimentally assigned N7-protonated O6-hydrogenated radical has HFCCs remarkably similar to those calculated for the guanine cation, which could be formed through net N7 hydrogen removal from the parent molecule.

The only dehydrogenated radical that was reported experimentally for the N7-protonated parent molecule is the radical formed via net hydrogen removal from the N9 position. This radical was observed in guanine hydrochloride monohydrate³⁹ and guanine hydrochloride dihydrate crystals.⁴¹ On average the spin density was determined to be 0.19 and 0.08 on N7 and N2, respectively. The calculated spin density distribution (0.10 and 0.13 on N7 and N2) is in acceptable agreement with experiment, but the results are not spectacular. Comparison of calculated (Table 12) and experimental (Table 9) HFCCs for the N9-dehydrogenated radical cation indicates that this radical is unlikely to be responsible for the observed spectrum. In order to account for possible differences in the hydrogen-bonding scheme to N7, the variation in the HFCCs with respect to the N7–H bond length for the protonated N9-dehydrogenated radical was investigated, as previously discussed for the protonated O6-hydrogenated radical. The results from this study are displayed in Table 14. The amino hydrogen couplings did not change with a variation in the N7–H bond length and, thus, the results were not recorded in the table. The C8–H couplings

also do not change very much upon elongation of the N7–H bond. The variation in the N7 hydrogen HFCCs is the greatest, but the calculated N7–H coupling is still not in agreement with that obtained experimentally.

Contrary to the spin density in the N7-protonated N9-dehydrogenated radical, the spin density in the nonprotonated N9-dehydrogenated radical is very similar to that assigned experimentally to the protonated radical form. In particular, the calculated spin density distribution yields 0.14 and 0.08 on N7 and N2, respectively (experimental values N7 0.19 and N2 0.08). The experimental N7–H anisotropic tensor (–3.7, –1.5, 5.1 G) is in excellent agreement with that calculated for C8–H in the nonprotonated radical (–3.7, –0.7, 4.4 G) but, as previously mentioned, in poor agreement with the N7–H HFCC calculated for the protonated radical (–2.2, –1.1, 3.3 G). In addition, the two experimental N2–H anisotropic couplings (–1.4, –0.5, 1.9 G and –1.7, –0.4, 2.1 G) are in excellent agreement with the two N2–H couplings obtained for the nonprotonated N9-dehydrogenated radical (–1.5, –0.9, 2.4 G and –2.2, –0.6, 2.8 G). The corresponding anisotropic tensors for the N7-protonated radical are (–2.1, –1.1, 3.2 G) and (–3.1, –0.8, 3.9 G). Thus, it can be concluded that the experimentally assigned N7-protonated N9-dehydrogenated radical is, in reality, most probably the corresponding nonprotonated radical. However, mistaking a C8–H coupling for an N7–H coupling, experimentally, is highly unlikely. No other possibilities can be put forth for the observed radical at this time through the comparison of the experimental couplings and those calculated in the present study.

Two different N7-protonated hydroxylated radicals have been observed experimentally which are formed through addition of a hydroxyl radical to the C5 and C8 positions. The C8-hydroxylated radical was calculated to be the lowest energy radical lying 20.5 kcal/mol lower in energy than the corresponding C5 radical. The relative order of these two hydroxylated radicals is similar to that discussed for the nonprotonated radicals where the C5-hydroxylated radical is 19.0 kcal/mol higher in energy than the C8-hydroxylated radical.

The protonated C5-hydroxylated radical was assigned to a spectrum observed in crystals of guanine hydrobromide monohydrate.²⁰ The experimental spin density was determined to be 0.13, 0.11, and 0.12 on C8, N7, and N2, respectively, whereas the main components of the calculated spin density are 0.29, 0.12, and 0.37 on C8, C2 and C4, respectively (Table 11). Clearly, the experimental and calculated spin density distributions are not in agreement. Analysis of the experimental (Table 9) and the calculated (Table 12) HFCCs indicates that the C5-hydroxylated radical is more than likely not responsible for the observed spectrum. In particular, the calculated C8–H anisotropic HFCC is approximately 3 G larger than those recorded from the experiments and the other couplings also do not correspond.

Other possibilities were discussed for the radical assigned to structure V in ref 20, including the C5-hydrogenated and the N9-dehydrogenated radical. The C5-hydrogenated radical was concluded to be unlikely since a large C5–H coupling would be expected. This is confirmed by the C5–H HFCCs calculated for the nonprotonated C5-hydrogenated radical (Table 6), which has an isotropic component of 49.5 G. The possibility that the recorded HFCCs were due to the N7-protonated N9-dehydrogenated radical was also dismissed since the spectrum observed in the crystals of guanine:HBr:H₂O was different from the spectrum observed in other crystal studies which was assigned to this radical (Table 9). However, it was concluded in the present study that the previous assignments of the protonated

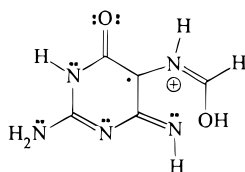


Figure 2. Molecular structure of the ring-opened, N7-protonated guanine radical cation.

N9-dehydrogenated radical were most probably incorrect and that the C5-hydrogenated and hydroxylated radicals are not leading to the spectrum recorded for guanine:HBr:H₂O. Thus, comparison of the experimental results assigned to the N7-protonated C5-hydroxylated radical (Table 9) and the calculated HFCCs for the N7-protonated N9-dehydrogenated radical (Table 12) is in order.

The experimentally assigned C5-hydroxylated couplings consist of C8–H isotropic (−3.7 G) and anisotropic (−1.9, −0.5, 2.4 G) couplings which are in excellent agreement with the C8–H couplings calculated for the N9-dehydrogenated radical ($A_{\text{iso}} = -2.9$ G; $T_{ii} = -1.7, -0.6, 2.3$ G). The experimental “C5-hydroxylated” N7–H couplings ($A_{\text{iso}} = -3.2$ G; $T_{ii} = -2.4, -1.0, 3.4$ G) and the calculated N7–H couplings in the N9-dehydrogenated radical ($A_{\text{iso}} = -2.8$ G; $T_{ii} = -2.2, -1.1, 3.3$ G) are also in excellent agreement. In addition, both the experimental and the calculated radicals under discussion exhibit two N2–H couplings, with isotropic contributions of approximately −3.5 G and significant anisotropic tensors. Through this comparison, it can be determined that the observed radical which was originally assigned to the C5-hydroxylated radical is in reality the N9-dehydrogenated radical. It should also be noted that much better agreement is obtained between the N9-dehydrogenated calculated HFCCs and the experimental C5-hydroxylated HFCCs than with the experimental “N9-dehydrogenated” couplings discussed previously.

The final hydroxylated radical cation, which has been observed in experimental studies, is that formed by net hydroxyl radical addition to the C8 position. This radical was observed in single crystals of guanine hydrochloride dihydrate.⁴¹ The observed spectrum consists of a large C8–H isotropic coupling (20.2 G) and a very small anisotropic tensor (−1.1, −0.6, 1.6 G). This is in excellent agreement with the calculated coupling for the C8 hydrogen ($A_{\text{iso}} = 17.5$ G; $T_{ii} = -0.9, -0.5, 1.4$ G). Experimentally, another relatively large isotropic coupling was observed for the hydrogen attached to the N7 position (−8.5 G) which also possessed a large anisotropy (−6.5, −1.5, 8.0 G). The calculated N7–H couplings ($A_{\text{iso}} = -7.0$ G; $T_{ii} = -5.9, -1.7, 7.6$ G) are also in agreement with experiment. A small N9–H coupling was also noted for this radical (experimental and calculated isotropic HFCCs of −2.2 and −2.1 G, respectively). Experimentally, it was speculated that the observed spectrum could be due to the C8-hydrogenated radical where the additional hydrogen is added to an in-plane position and, thus, only one large C8–H coupling is observed. This alternative seems very unlikely due to the excellent agreement between experimental and calculated HFCCs for the C8-hydroxylated radical cation. Hence, the experimental assignment is supported by the calculations.

One last radical observed experimentally was thought to have a molecular structure very similar to the N7-protonated C8-hydroxylated radical.²⁰ One experimental coupling was observed which was assigned to a C8 hydrogen which underwent significant reorientation. The radical was proposed to be the N7-protonated ring-opened radical (Figure 2). This radical was calculated to be 28.8 kcal/mol higher in energy than the

corresponding ring-closed radical. The experimental coupling consisted of an isotropic (−4.9 G) and an anisotropic (−2.6, 0.1, 2.4 G) C8–H coupling. These results are in good agreement with the C8–H couplings calculated for this radical ($A_{\text{iso}} = -4.8$ G; $T_{ii} = -2.5, -0.5, 3.0$ G). In addition to the C8–H HFCC, the calculations indicate that a larger coupling should be observed for the hydrogen attached to N9, as well as smaller couplings for the hydrogens attached to N1, N7, and O8. A more detailed experimental study is required for a definitive identification of this radical.

Conclusion

The geometries, the spin density distributions, and the hyperfine coupling constants in radicals that are possible radiation products in guanine have been studied through the use of density functional theory. Possible hydrogenated, dehydrogenated, and hydroxylated radicals were examined and the coupling constants were compared to those obtained from detailed ESR/ENDOR studies on single crystals of numerous guanine derivatives. In addition to the neutral radicals, various protonated radicals were also examined. These radicals involved mainly protonation at the N7 position and are important to study in order to transfer results obtained from single crystals to full DNA.

The guanine anion was determined to undergo major geometrical distortions upon formation. Calculated spin densities and HFCCs were not consistent with the experimental results for the radical identified as the guanine anion. This disagreement is likely due to the distortion observed for the theoretical geometry. If the geometry of the anion is constrained to a planar geometry, the agreement between theory and experiment improves slightly. However, the couplings of the O6-hydrogenated radical match the experimental results assigned to the anion more closely. Experimentally, the anion and its O6-protonated form can be distinguished through the identification of the amino hydrogen HFCCs. The geometry of the cation, on the other hand, was optimized to a planar form. Similar to the guanine anion, the experimental and the calculated HFCCs were not in good agreement. It was concluded that more detailed experimental, as well as theoretical, investigations are required in order to identify either the guanine anion or the guanine cation.

The N9-dehydrogenated radical was determined to be the lowest energy radical in this class with the corresponding N1 and N2 radicals very close in energy. Only the N2-dehydrogenated radical has been previously observed experimentally and the calculated HFCCs confirm the experimental assignment of this radical. The C8- and C5-hydrogenated radicals are the lowest and highest energy radicals in their class. Both of these radicals have been observed experimentally and the calculations support their assignment. The C8-hydroxylated radical is the lowest energy radical formed via net hydroxyl radical addition. The C4- and C5-hydroxylated radicals, in addition to the corresponding hydrogenated radicals, adopt a butterfly conformation upon optimization, which agrees with observations made in previous theoretical studies. The couplings assigned to the C4-hydroxylated radical experimentally are only in fair agreement with the calculated values.

The good agreement obtained between theory and experiment for the nonprotonated radicals is not immediately transferable to the N7-protonated guanine radicals investigated in the present study. Of the protonated radicals examined, only the experimental assignments of the C8-hydrogenated and C8-hydroxylated radicals are supported by the calculations. The spectrum

experimentally assigned to the protonated O6-hydrogenated radical was speculated to arise from an averaging of the planar forms of the protonated and nonprotonated O6-hydrogenated radicals. In addition, it was also noted that the spectrum experimentally assigned to the N7-protonated O6-hydrogenated radical contains HFCCs very similar to the guanine cation. The protonated N9-dehydrogenated radical was concluded to be unlikely responsible for the observed spectrum assigned experimentally to this radical. The only radical possessing couplings similar to those observed experimentally are the nonprotonated N9-dehydrogenated radical, but it was deemed unlikely to mistake a N7–H coupling for a C8–H coupling. No other possible products could be identified as leading to the experimental HFCCs. In addition, the observed HFCCs thought to arise from the C4- and the C5-hydroxylated radicals were determined to originate from other guanine radicals. It was concluded that more experimental, as well as theoretical, studies are required for the full identification of N7-protonated radicals generated upon irradiation of guanine derivatives. It should be noted that no environmental effects were included in present study. This offers a possible explanation for discrepancies between theory and experiment.

Acknowledgment. We gratefully acknowledge the Natural Sciences and Engineering Research Council of Canada (NSERC), the Swedish Natural Science Research Council (NFR), and the Killam Trust for financial support. We also thank the Computing and Network Services at the University of Alberta for grants of computer time.

Supporting Information Available: The molecular geometries in Cartesian coordinates for all radicals in the present study are available (6 pages). Ordering information is given on any current masthead page.

References and Notes

- (1) Gräslund, A.; Ehrenberg, A.; Rupprecht, A.; Ström, G. *Biochim. Biophys. Acta* **1971**, 254, 172.
- (2) Gräslund, A.; Ehrenberg, A.; Rupprecht, A.; Ström, G.; Crespi, H. *Int. J. Radiat. Biol.* **1975**, 8, 313.
- (3) Hüttermann, J.; Voit, K.; Oloff, H.; Köhnlein, W.; Gräslund, A.; Rupprecht, A. *Faraday Discuss. Chem. Soc.* **1984**, 78, 135.
- (4) Hüttermann, J. In *Radical Ionic Systems*; Lund, A., Shiotani, M., Eds.; Kluwer Academic: Boston, MA, 1991.
- (5) Bernhard, W. A. *J. Phys. Chem.* **1989**, 93, 2187.
- (6) Sevilla, M. D.; Becker, D.; Yan, M.; Summerfield, S. R. *J. Phys. Chem.* **1991**, 95, 3409.
- (7) Dizdaroglu, M.; Gajewski, E.; Reddy, P.; Margolis, S. A. *Biochemistry* **1989**, 28, 3625.
- (8) Olinski, R.; Briggs, R. C.; Hnilica, L. S.; Stein, J.; Stein, G. *Radiat. Res.* **1981**, 86, 102.
- (9) Gajewski, E.; Dizdaroglu, M. *Biochemistry* **1990**, 29, 977.
- (10) Prakash Rao, P. J.; Bothe, E.; Schulte-Frohlinde, D. *Int. J. Radiat. Biol.* **1992**, 61, 577.
- (11) Close, D. M. *Radiat. Res.* **1993**, 135, 1.
- (12) Sagstuen, E.; Hole, E. O.; Nelson, W. H.; Close, D. M. *Radiat. Res.* **1998**, 149, 120.
- (13) Sagstuen, E.; Hole, E. O.; Nelson, W. H.; Close, D. M. *Radiat. Res.* **1996**, 146, 425.
- (14) Malkin, V. G.; Malkina, O. L.; Eriksson, L. A.; Salahub, D. R. In *Modern Density Functional Theory, A Tool for Chemistry*; Seminario, J. M., Politzer, P., Eds.; Elsevier: New York, 1995.
- (15) Engels, B.; Eriksson, L. A.; Lunell, S. *Adv. Quantum Chem.* **1997**, 27, 297.
- (16) Wetmore, S. D.; Boyd, R. J.; Eriksson, L. A. *J. Phys. Chem. B* **1998**, 102, 5369.
- (17) Wetmore, S. D.; Himo, F.; Boyd, R. J.; Eriksson, L. A. *J. Phys. Chem. B* **1998**, 102, 7484.
- (18) Wetmore, S. D.; Eriksson, L. A.; Boyd, R. J. *J. Phys. Chem. B*, in press.
- (19) Wetmore, S. D.; Boyd, R. J.; Eriksson, L. A. *J. Phys. Chem. B* **1998**, 102, 7674.
- (20) Hole, E. O.; Sagstuen, E.; Nelson, W. H.; Close, D. M. *Radiat. Res.* **1991**, 125, 119.
- (21) Hole, E. O.; Nelson, W. H.; Sagstuen, E.; Close, D. M. *Radiat. Res.* **1992**, 129, 119.
- (22) Hole, E. O.; Sagstuen, E.; Nelson, W. H.; Close, D. M. *Radiat. Res.* **1992**, 129, 1.
- (23) The original three-parameter hybrid suggested by Becke can be found in Becke, A. D. *J. Chem. Phys.* **1993**, 98, 1372. A slightly modified form implemented in the Gaussian programs can be found in: Stephens, P. J.; Devlin, F. J.; Chabowski, C. F.; Frisch, M. J. *J. Phys. Chem.* **1994**, 98, 11623.
- (24) Lee, C.; Yang, W.; Parr, R. G. *Phys. Rev. B* **1988**, 37, 785.
- (25) Ditchfield, R.; Hehre, W. J.; Pople, J. A. *J. Chem. Phys.* **1971**, 54, 724. Hehre, W. J.; Ditchfield, R.; Pople, J. A. *J. Chem. Phys.* **1972**, 56, 2257. Hariharan, P. C.; Pople, J. A. *Mol. Phys.* **1974**, 27, 209. Gordon, M. S. *Chem. Phys. Lett.* **1980**, 76, 163. Hariharan, P. C.; Pople, J. A. *Theor. Chim. Acta* **1973**, 28, 213. McLean, A. D.; Chandler, G. S. *J. Chem. Phys.* **1980**, 72, 5639. Krishnan, R.; Binkley, J. S.; Seeger, R.; Pople, J. A. *J. Chem. Phys.* **1980**, 72, 650. Clark, T.; Chandrasekhar, J.; Spitznagel, G. W.; Schleyer, P. v. R. *J. Comput. Chem.* **1983**, 4, 294. Frisch, M. J.; Pople, J. A.; Binkley, J. S. *J. Chem. Phys.* **1984**, 80, 3265.
- (26) Bauschlicher, C. W., Jr.; Partridge, H. *J. Chem. Phys.*, **1995**, 103, 1788.
- (27) Frisch, M. J.; Trucks, G. W.; Schlegel, H. B.; Gill, P. M. W.; Johnson, B. G.; Robb, M. A.; Cheeseman, J. R.; Keith, T. A.; Petersson, G. A.; Montgomery, J. A.; Raghavachari, K.; Al-Laham, M. A.; Zakrzewski, V. G.; Ortiz, J. V.; Foresman, J. B.; Cioslowski, J.; Stefanov, B. B.; Nanayakkara, A.; Challacombe, M.; Peng, C. Y.; Ayala, P. Y.; Chen, W.; Wong, M. W.; Andres, J. L.; Replogle, E. S.; Gomperts, R.; Martin, R. L.; Fox, D. J.; Binkley, J. S.; Defrees, D. J.; Baker, J.; Stewart, J. P.; Head-Gordon, M.; Gonzalez, C.; Pople, J. A. *Gaussian 94* (Revision B.2); Gaussian, Inc.: Pittsburgh, PA, 1995.
- (28) Perdew, J. P.; Wang, Y. *Phys. Rev. B* **1986**, 33, 8800.
- (29) (a) Perdew, J. P. *Phys. Rev. B* **1986**, 33, 8822. (b) Perdew, J. P. *Phys. Rev. B* **1986**, 34, 7406.
- (30) Amant, A.; Salahub, D. R. *Chem. Phys. Lett.* **1990**, 169, 387. St-Amant, A. Ph.D. Thesis, Université de Montréal, 1991. Salahub, D. R.; Fournier, R.; Mlynarski, P.; Papai, I.; St-Amant, A.; Ushio, J. In *Density Functional Methods in Chemistry*; Labanowski, J., Andzelm, J., Eds.; Springer: New York, 1991.
- (31) Orlov, V. M.; Smirnov, A. N.; Varshavsky, Y. M. *Tetrahedron Lett.* **1976**, 48, 4377.
- (32) Colson, A. O.; Sevilla, M. D. *Int. J. Radiat. Biol.* **1995**, 67, 627.
- (33) Close, D. M.; Sagstuen, E.; Nelson, W. H. *J. Chem. Phys.* **1985**, 82, 4386.
- (34) Close, D. M.; Nelson, W. H.; Sagstuen, E. *Radiat. Res.* **1987**, 112, 283.
- (35) Kim, H.; Budzinski, E. E.; Box, H. C. *J. Chem. Phys.* **1989**, 90, 1448.
- (36) Hole, E. O.; Nelson, W. H.; Close, D. M.; Sagstuen, E. *J. Chem. Phys.* **1987**, 86, 5218.
- (37) Colson, A. O.; Sevilla, M. D. *J. Phys. Chem.* **1996**, 100, 4420.
- (38) Hole, E. O.; Sagstuen, E. *Radiat. Res.* **1987**, 109, 190.
- (39) Close, D. M.; Sagstuen, E.; Nelson, W. H. *Radiat. Res.* **1988**, 116, 379.
- (40) Sagstuen, E.; Hole, E. O.; Nelson, W. H.; Close, D. M. *Radiat. Res.* **1988**, 116, 196.
- (41) Nelson, W. H.; Hole, E. O.; Sagstuen, E.; Close, D. M. *Int. J. Radiat. Biol.* **1988**, 54, 963.